Fang *et al. Bioresour. Bioprocess.* (2020) 7:5
https://doi.org/10.1186/s40643-019-0293-1

Bioresources and Bioprocessing

RESEARCH Open Access

Astaxanthin accumulation difference between non-motile cells and akinetes of *Haematococcus pluvialis* was affected by pyruvate metabolism

Lei Fang, Jingkui Zhang, Zhongnan Fei and Minxi Wan*

Abstract

Background: *Haematococcus pluvialis* is the best source of natural astaxanthin, known as the king of antioxidants. *H. pluvialis* have four cell forms: spore, motile cell, non-motile cell and akinete. Spores and motile cells are susceptible to photoinhibition and would die under photoinduction conditions. Photoinduction using non-motile cells as seeds could result in a higher astaxanthin production than that using akinetes. However, the mechanism of this phenomenon has not been clarified.

Results: Transcriptome was sequenced and annotated to illustrate the mechanism of this phenomenon. All differentially expressed genes involved in astaxanthin biosynthesis were up-regulated. Particularly, *chyb* gene was up-regulated by 16-fold, improving the conversion of *β*-carotene into astaxanthin. Pyruvate was the precursor of carotenoids biosynthesis. Pyruvate kinase gene expression level was increased by 2.0-fold at the early stage of akinetes formation. More changes of gene transcription occurred at the early stage of akinetes formation, 52.7% and 51.9% of total DEGs in control group and treatment group, respectively.

Conclusions: Genes transcription network was constructed and the synthesis mechanism of astaxanthin was clarified. The results are expected to further guide the in-depth optimization of the astaxanthin production process in *H. pluvialis* by improving pyruvate metabolism.

Keywords: Astaxanthin, *Haematococcus pluvialis*, Pyruvate, Transcriptome

Background

Astaxanthin is regarded as the best biological antioxidant. Its antioxidant activity is 10, 65, 100 and 550 times of *β*-carotene, vitamin C, *α*-tocopherol, and vitamin E, respectively (García-Malea et al. 2006; Olaizola 2000; Ranjbar et al. 2008; Zhang et al. 2009). As the best source of natural astaxanthin, *Haematococcus pluvialis* could accumulate 4–5% astaxanthin of dry weight under certain conditions (Wan et al. 2015). Industrial production of *H. pluvialis* was successfully achieved by a two-stage model. First stage is cell proliferation phase (also called the growth phase), in which the algae cells grow rapidly until to a high cell density. The second stage is photoinduction stage, aiming to promote the accumulation of astaxanthin in *H. pluvialis* (He et al. 2007; Lorenz and Cysewski 2000).

Previous studies mainly focused on the optimization of the second stage to improve astaxanthin accumulation ability. Temperature (Wan et al. 2014b), strong light (Lv et al. 2016), high salinity (Sarada et al. 2002), plant hormone (Gao et al. 2012a), nitrogen deprivation (Wang et al. 2013), oxygen stress (Gu et al. 2013), metal ion stress (Yu et al. 2015) and ethanol (Wen et al. 2015) were reported in the second stage to promote *H. pluvialis*

*Correspondence: wanminxi@ecust.edu.cn
State Key Laboratory of Bioreactor Engineering, East China University of Science and Technology, Mail Box 301, Meilong Road 130, Shanghai 200237, People's Republic of China

accumulate astaxanthin. Li et al. (2019a) and Choi et al. (2011) have shown that the appropriate cell type for photoinduction was the non-motile cell, however, there was no article has interpreted this mechanism.

Transcriptome sequencing was regarded as an efficient approach for exploring the mechanism of astaxanthin accumulation. The gene transcription changes of *H. pluvialis* have been discussed in many studies, e.g., high light intensity could increase the activity of *β*-carotene ketolase (BKT) and IPP isomerase (Linden 1999); astaxanthin synthesis-related genes were significantly up-regulated in *H. pluvialis* mutant under 15% CO_2 (Li et al. 2017); the astaxanthin accumulation ability of *H. pluvialis* could be improved by gibberellin (GA3), accompanied by increasing the transcription of *ipi* (isopentenyl pyrophosphate isomerase), *psy* (phytoene synthase), *pds* (phytoene desaturase) and *bkt* genes (Gao et al. 2013). However, these researches were mainly focused on the regulation mechanism of astaxanthin synthesis responding to various stresses, e.g., light, salinity, temperature, hormone, iron and inorganic carbon (Lee et al. 2016; Wen et al. 2015).

The direct precursor of fatty acid biosynthesis is acetyl-CoA (Shtaida et al. 2015). Acetyl-CoA carboxylase (ACACA) can enhance the carboxylation of acetyl-CoA to malonyl-CoA (Shtaida et al. 2015). This step was considered a critical step in the lipid biosynthetic pathway (Huerlimann and Heimann 2013). Lipid can be used for the esterification of astaxanthin (Karsten et al. 2009; Schoefs et al. 2001). Pyruvate metabolism plays an important role in glycolysis to form acetyl-CoA. Cheng et al. (2017) reported that most significant differences were found in unigenes related to photosynthesis, carotenoid biosynthesis and fatty acid biosynthesis pathways when photoinduction with high light under 15% CO_2. Above studies indicated astaxanthin synthesis mechanism is complicated and has not been systematically clarified.

To understand the molecular mechanism of astaxanthin synthesis and to dissect the mechanism that photoinduction using non-motile cells as seeds could result in a higher astaxanthin production than that of using akinetes, transcriptome sequencing of microalgae culture process was conducted. The metabolic network between astaxanthin synthesis and pyruvate metabolism was proposed. The mechanism by which high astaxanthin production was obtained by non-motile cells as seeds was dissected. The results provide a new entry point to improve the astaxanthin productivity.

Methods

Algal strains

Haematococcus pluvialis ZY-18 was obtained from State Key Laboratory of Bioreactor Engineering, East China University of Science and Technology (Shanghai, China).

Seed culture conditions

The basic seed medium and culture methods were the same with Hata et al. (2001). *H. pluvialis* cells were obtained from broths at different incubation times. *H. pluvialis* cells were used for the next step in photoinduction experiments.

Photoinduction culture conditions

Haematococcus pluvialis cells from cell proliferation phase were inoculated to the NIES-N medium (Kang et al. 2005) and then were turned into the photoinduction stage. The initial cell concentration was approximately 0.3 g/L in all the experiments. 1-L column bioreactors (height: 45 cm, and diameter: 7 cm) for photoinduction was a cylindrical glass tube with a conical bottom (height: 6 cm). 5% CO_2 mixing was conducted by sparging air supplemented with a flow rate of 0.2 L/min. A gas sparger was centrally placed at the bottom. Throughout the experiment, the light intensity was about 540 μmol/(m^2 s) (Wan et al. 2014b) and the culture temperature was controlled at 28 °C. All experiments have two biological replicates.

Measurement of dry weight

V ml broth containing algal cells was obtained by centrifuging the culture at 2683×g for 10 min, and collected into an empty tumbler (W_1) after being washed twice with distilled water and then dried at 85 °C for 24 h (W_2). The dry weight was calculated in terms of the equation:

$$C_x = (W_2 - W_1)/V \times 1000, \quad (1)$$

where C_x (g/L) is dry weight of broth, W_1 is the weight of the empty tumbler, and W_2 (g) is the weight after being dried, and V (ml) is the volume of the initial sample, respectively.

Determination of astaxanthin content

The astaxanthin content was measured by a modified Boussiba method (Borowitzka et al. 1991; Wan et al. 2014a). V ml culture sample was centrifuged for 10 min at 2683×g. 4–6 pieces of glass beads and 1 ml of dimethyl sulfoxide were added to each centrifuge tube, and subsequently were vortex oscillated for 30 s, and then heated with 45 °C water bathing for 15 min. Later, 1 ml acetone was added into the mixture solution and centrifuged for 10 min at 2683×g. Then the supernatant was collected and transferred into a volumetric flask. Above-mentioned acetone extraction and supernatant collection were conducted repeatedly until the supernatant becomes transparent and the precipitate becomes white. The absorbance values of the extracts were determined at 474 nm using acetone as reference.

The astaxanthin content was calculated in terms of the equation:

$$C_{\mathrm{Car}} = \mathrm{OD}_{474} \times V_1/V_2 \times \text{dilution ration}/210, \quad (2)$$

$$C_{\text{Asta content}} = C_{\mathrm{car}}/C_{\mathrm{x}} \times 85, \quad (3)$$

where C_{Car} is the concentration of carotenoid (mg/L), Cx is the dry weight of the algal (g/L) and $C_{\text{Asta content}}$ is the content (%) of astaxanthin, V_1 is the volume of the volumetric flask (ml), and V_2 is the volume of the initial sample (ml).

RNA isolation, cDNA library preparation, qRT-PCR and sequencing

Totally, the transcription profiling of samples at six time points were evaluated, with two biological replicates at each time point. In the proliferation stage, three samples in different time points were selected: (1) Sample 1, cells at 100 h (green motile cells accounted for the vast majority); (2) Sample 2, cells at 250 h (non-motile cells accounted for the vast majority); (3) Sample 3, cells at 550 h (brown akinetes accounted for the vast majority). In the photoinduction phase, three samples were also selected as follows: (1) Sample 4, Sample 2 cells were transferred to weak light for 0.5 day under photoinduction condition (green non-motile cells were converted to brown akinetes); (2) Sample 5, Sample 3 cells were transferred and exposed to weak light for 6 days under photoinduction condition (red akinetes accounted for the majority, astaxanthin content was high, and astaxanthin content was no longer increased); (3) Sample 6 was the Sample 4 cells continued photoinduction until the 6th day (red akinetes account for the vast majority. The astaxanthin content was high, and the astaxanthin content was no longer increased). Therefore, there are two cultivation routes named treatment group (green non-motile cells were used for photoinduction in the order: Sample 1, 2, 4 and 6) and control group (brown akinetes were used for photoinduction in the order: Sample 1, 2, 3 and 5). Total RNA of each sample was extracted and mRNA was purified. Then the cDNA library was constructed.

The gene-specific primers were designed using Primer 5 software (Additional file 1: Table S1). qRT-PCR analysis of related genes was conducted according to Gao et al. (2012b). The data were analyzed using the comparative Ct ($2^{-\Delta\Delta CT}$) method according to Livak and Schmittgen (2000).

The cDNA library subjected to paired-end (PE) sequencing based on the Illumina NextSeq 500 sequencing platform by Shanghai Personal Biotechnology Company. All sequencing data reported in this paper have been deposited in the NODE (National Omics Data Encyclopedia). The accession numbers for RPKM and annotation results are NODE: OEP000493.

Transcriptome mapping, annotation, and differential transcription analysis

The software of cut-adapt was used to remove adapters, poly-N strands, and low-quality reads. Then all filtered reads were examined by FastQC (http://www.bioinformatics.babraham.ac.uk/projects/fastqc/) to confirm data quality. Transcript assembly used Trinity with a K-mer 25 bp. Every transcript was compared with the NCBI non-redundant protein database and eggNOG (evolutionary genealogy of genes: non-supervised Orthologous Groups) using the Blast algorithm (version 2.2.30+). Transcripts with same gi number were classified as a unigene and only the longest transcript was kept. After that, filtered reads were mapped to unigenes with Bowtie2 (v2.2.4) and the reads per kilobase of exon model per million (RPKM) mapped fragments was used to represent gene transcription.

Differential transcription analysis between samples was conducted using the R package, DEGseq (version 1.18.0). Genes with $|\text{fold changes}| > 2$ and P value < 0.05 were considered as statistically significant. Functional analysis of differential transcription genes was performed by Gene ontology (GO) and Kyoto Encyclopedia of Genes and Genomes (KEGG) enrichment analysis. GO

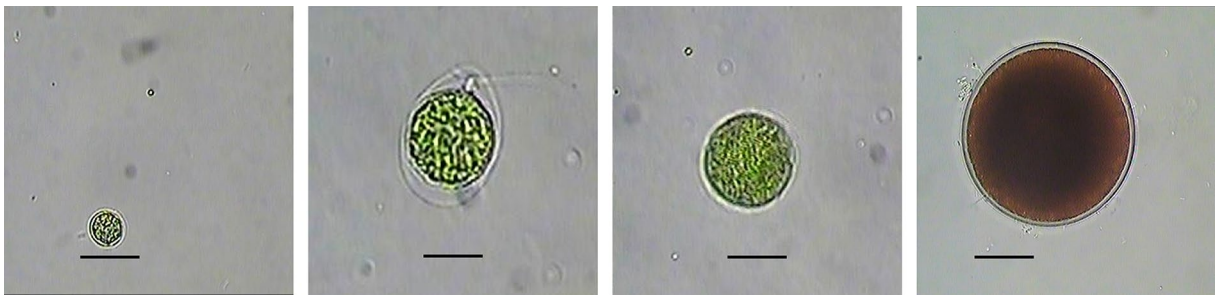

Fig. 1 Four cell types of *H. pluvialis*. From left to right represents spores, motile cells, non-motile cells and akinetes. Bar = 20 μm

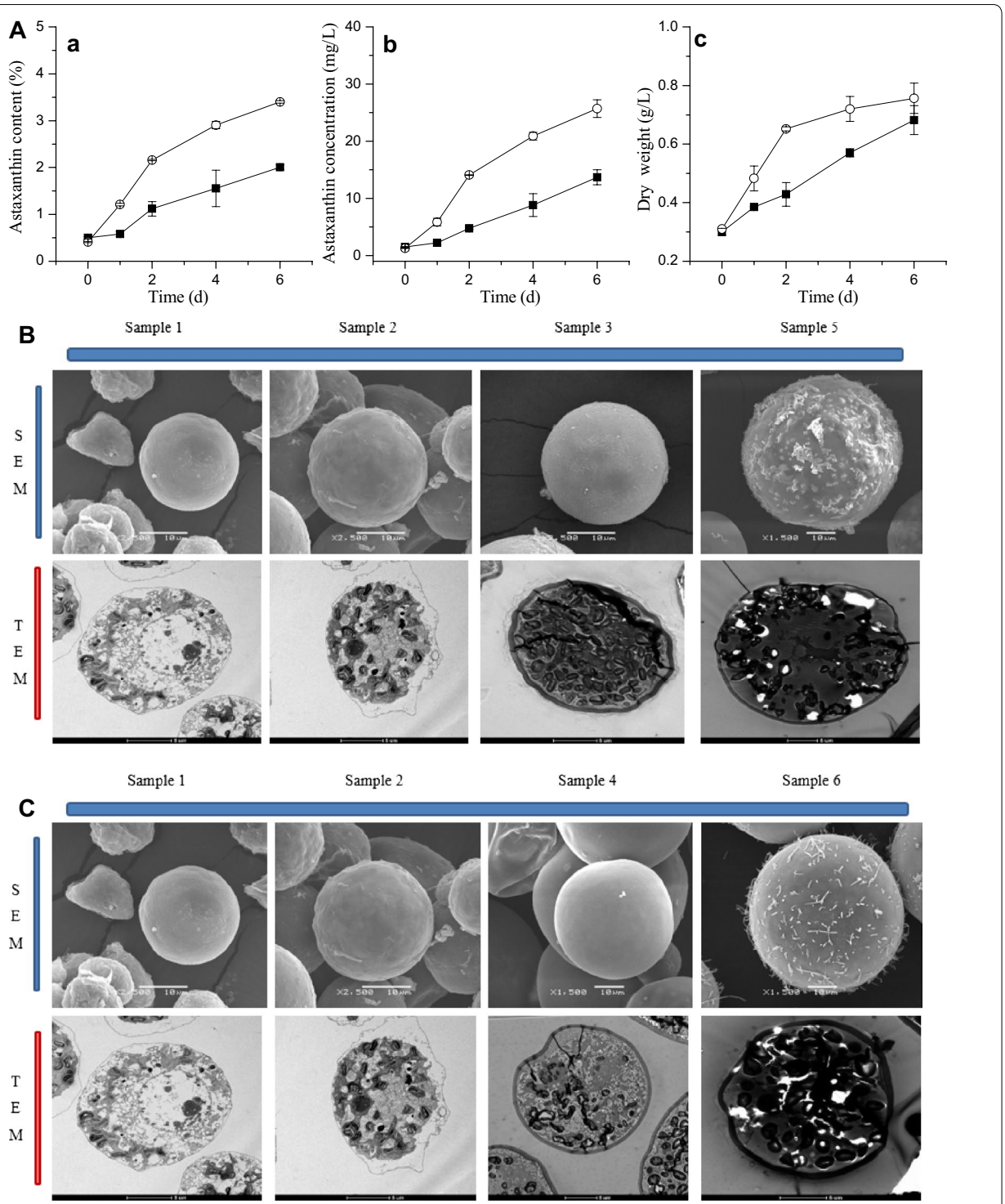

Fig. 2 Induction effect and images of *H. pluvialis* using different cell type as seeds. **A** Induction effect of *H. pluvialis* using different cell type as seeds. **a** Astaxanthin content during induction process; **b** astaxanthin concentration during induction process, **c** dry weight during induction process. Hollow circle represents green non-motile cells as seeds, and solid square represents brown akinetes as seeds; **b**, **c** represent SEM and TEM images of control group (**B**, 1235 route) and treatment group (**C**, 1246 route), respectively. Sample 1, Sample 2 and Sample 3 were the heterotrophic cells at 100 h, 250 h, and 550 h, respectively; Sample 4 was Sample 2 cells induction for 0.5 day; Sample 5 was Sample 3 cells induction for 6 days; Sample 6 was the Sample 2 cells induction for 6 days. SEM: scanning electron microscope (scale bar = 10 μm); TEM: transmission electron microscope (scale bar = 5 μm). Data are shown as mean ± SD, and number of replications is two ($n = 2$)

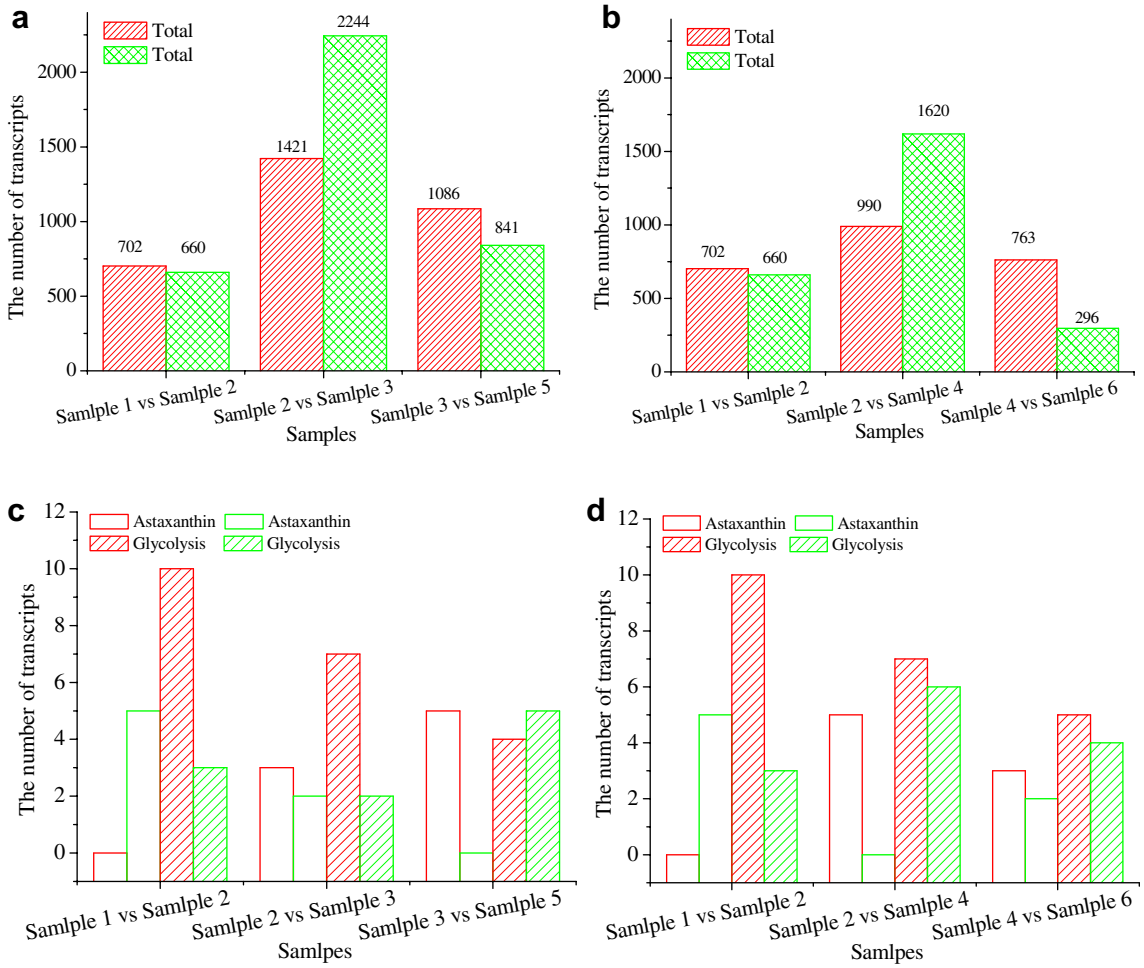

Fig. 3 Transcription amounts of up/down-regulation genes at different time points. **a**, **b** represent the number of total genes in control group (**a**, 1235 route) and treatment group (**b**, 1246 route), respectively; **c**, **d** represent the number of astaxanthin genes and glycolysis genes in control group (**c**) and treatment group (**d**). Sample 1, Sample 2 and Sample 3 were the heterotrophic cells at 100 h, 250 h, and 550 h, respectively; Sample 4 was Sample 2 cells induction for 0.5 day; Sample 5 was Sample 3 cells induction for 6 days; Sample 6 was the Sample 2 cells induction for 6 days. Red and green present up- and down-regulation genes number, respectively

analysis of each unigene was carried out using Blast2go software and KEGG enrichment analysis was performed using KASS and KEGG automatic annotation server, respectively.

Statistical analysis

All exposure experiments were repeated two times independently, and data were recorded as the mean with standard deviation (SD). For mRNA-sequencing were analyzed with the two biological replicates. Statistical analyses were performed using the Spearman correlation analysis (SPSS19.0). For all of the data analysis, a P-value < 0.05 was considered as statistically significant.

Results and discussion

The comparison of photoinduction differences

Haematococcus pluvialis have four cell forms—spore, motile cell, non-motile cell and akinete (Fig. 1). To compare the photoinduction result of non-motile cells group and brown akinetes group, the astaxanthin content, astaxanthin concentration and dry weight were detected. Comparing with control group, a better photoinduction result was acquired using non-motile cells as seeds. The astaxanthin content and astaxanthin concentration of non-motile cells group were 3.40% and 25.7 mg/L, respectively (Fig. 2a). The results were much higher than those in brown akinetes group. Our previous studies showed that spores and motile cells were susceptible to photoinhibition and would die under photoinduction

conditions. Therefore, non-motile cells of heterotrophic culture are the best cell type for photoinduction. Li et al. (2019a) and Choi et al. (2011) also demonstrated that the appropriate cell type for photoinduction was the non-motile cells.

Scanning electron microscope (SEM, Fig. 2b, c) and transmission electron microscope (TEM, Fig. 2b, c) image of *H. pluvialis* were carried out during two culture stage to further explore the changes of non-motile cells and akinetes as photoinduction seeds. From the TEM images, more lipid drops were observed when using non-motile cells as seeds. Cheng reported that massive astaxanthin was esterified in the endoplasmic reticulum, and deposits in cytoplasmic lipid droplets to avoid the feedback inhibitor of carotenoids biosynthesis (Cheng et al. 2017). Thus, the result confirmed the better photoinduction result of non-motile cells.

The comparison of gene transcription differences

To have a comprehensive understanding of astaxanthin synthesis, transcriptome sequencing on microalgae sequence culture process was conducted. De novo assembly of transcriptomes revealed the genomic and transcriptional features of two culture routes (1235 route and 1246 route). A total of 0.3 billion clean reads, and 43,583 unigenes were generated, respectively. According to the standard of $p < 0.05$, 2455 upregulation and 2576 downregulation unigenes were identified in treatment group (1246 route, Fig. 3a), while 3209 upregulation and 3745 downregulation unigenes were identified in control group (1235 route, Fig. 3b). Among the differentially expressed genes, the number of upregulation genes in glycolysis declined during culture, while the number of upregulation genes in astaxanthin synthesis increased (Fig. 3c, d). The products of glycolysis can be used for astaxanthin synthesis. Therefore, the early stage of culture may be important for astaxanthin synthesis.

Transcriptome and pathway analysis involved in astaxanthin biosynthesis

The genes participated in carotenoid biosynthesis and astaxanthin synthesis have been fully studied (Lee et al. 2016; Wen et al. 2015). The conversion of geranylgeranyl-pp (GGPP) into astaxanthin synthesis is successively catalyzed by BKT, CHYB (*β*-carotene-3-hydroxylase), LCYB (lycopene beta cyclase), PSY and ZDS (*ζ*-carotene desaturase). These enzymes have been reported as essential enzymes in astaxanthin synthesis (Huang et al. 2006; Zhong et al. 2011).

The condensation of two GGPP molecules into phytoene is catalyzed by PSY. Compared with control, *psy* gene was up-regulated by 2.4-fold at the end of photoinduction (Table 1). The conversion of phytoene into *β*-carotene is successively catalyzed by ZDS and LCYB. The two genes were both up-regulated during photoinduction stage (Figs. 4, 5a, b). *β*-Carotene is the precursor of astaxanthin synthesis. The reactions catalyzed by BKT and CHYB are regarded as the rate-limiting steps. The *bkt* and *chyb* genes were both up-regulated during

Table 1 Annotation and transcription changes of significantly different unigenes related to astaxanthin, fatty acid, pyruvate metabolic pathway and photosynthesis

Gene name	Gene definition	KEGG	3 vs. 4		5 vs. 6	
			FC	*P*-value	FC	*P*-value
Astaxanthin biosynthesis pathway						
bkt	*β*-Carotene ketolase (EC 1.14.99.63)	K09836	3.8	**	1.9	***
chyb	*β*-Carotene 3-hydroxylase (EC 1.14.15.24)	K15746	16	***	2.6	***
lcyb	Lycopene beta cyclase (EC 5.5.1.19)	K06443	2.9	***	1.9	***
psy	15-cis-Phytoene/all-trans-phytoene synthase (EC 2.5.1.32)	K02291	2.4	***	2.4	***
zds	*ζ*-Carotene desaturase (EC 1.3.5.6)	K00514	2.7	***	2.0	***
Pyruvate metabolic pathway						
ppc	Phosphoenolpyruvate carboxylase (EC 4.1.1.31)	K01595	1.0	*	2.1	***
pdhD	Dihydrolipoamide dehydrogenase (EC 1.8.1.4)	K00382	1.6	***	1.7	***
PK	Pyruvate kinase (EC 2.7.1.40)	K00873	2.0	***	1.3	***
fumA, fumB	Fumarate hydratase, class I (EC 4.2.1.2)	K01676	0.50	***	1.6	***
MDH2	Malate dehydrogenase (NADP +) (EC 1.1.1.82)	K00051	0.90	*	1.5	***
pdhC	Pyruvate dehydrogenase E2 component (dihydrolipoamide acetyltransferase) (EC 2.3.1.12)	K00627	2.0	***	1.7	***
pdhA	Pyruvate dehydrogenase E1 component alpha subunit (EC 1.2.4.1)	K00161	0.50	***	1.1	*
NADP-ME	Malate dehydrogenase (oxaloacetate-decarboxylating) (NADP+) (EC 1.1.1.40)	K00029	1.1	*	1.8	***

*** indicates statistical significance at *P*-value ≤ 0.001; ** indicates statistical significance at *P*-value ≤ 0.005; * indicates statistical significance at *P*-value ≤ 0.05

photoinduction stage (Figs. 4, 5a, b). At the initial stage of akinetes formation, the gene transcription difference was much more obvious than that at the end of photoinduction compared with control (Fig. 3). The *chyb* gene transcription level was 16-fold up-regulated of the control at the early stage of akinete formation (Table 1). Li also showed that *psy*, *CrtO* (*β*-carotene oxidase) and *LcyB* have relatively large changes during the early stage of akinetes formation (Li et al. 2019b). The result indicated that the early stage of akinetes formation may be important for astaxanthin synthesis.

From Figs. 4, 5a, b, it can be known that all genes related to astaxanthin synthesis were lowly expressed in the cell proliferation phase and highly expressed in the photoinduction stage in both routes. Nevertheless, the transcription level of genes related to astaxanthin synthesis in treatment group (1246 route) was much higher than that in control group (1235 route) (Fig. 5 and Table 1). The results explained that the appropriate cell type for photoinduction was non-motile cells. The high astaxanthin synthesis ability of non-motile cells was attributed to the high transcription level of astaxanthin synthesis-related genes.

Lycopene is the common intermediate substrate for astaxanthin and lutein synthesis. During photoinduction stage, the upregulation of *lcyB* gene expression was accompanied by the downregulation of *lcyE* gene expression (Fig. 4). This phenomenon would decrease lutein metabolism competition for the lycopene, suggesting more carbon flow to astaxanthin rather than lutein. Gao

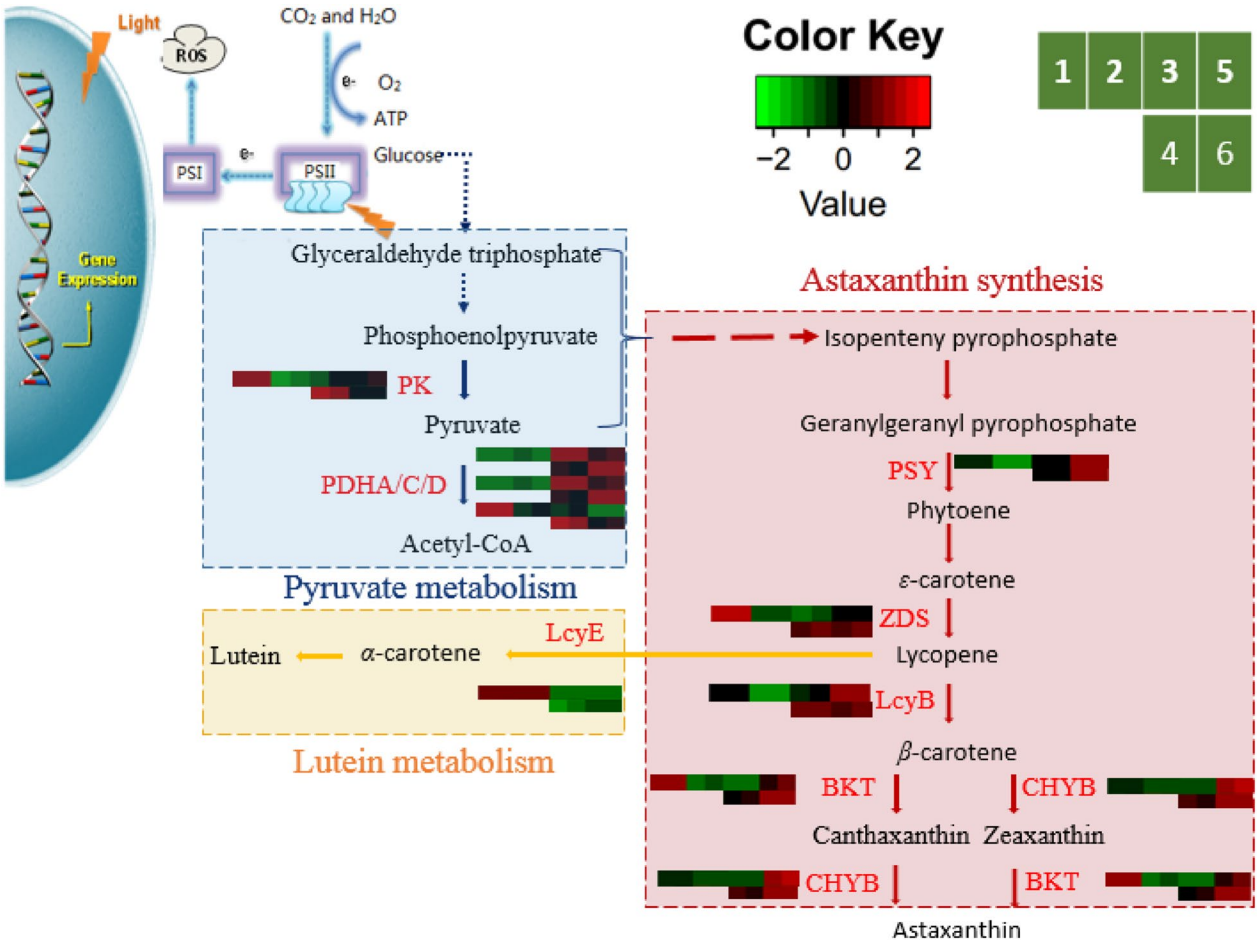

Fig. 4 The metabolism network and transcription regulation of astaxanthin metabolism. Deep red, dark blue and bright yellow background represent astaxanthin metabolism pathway, pyruvate metabolism pathway and lutein metabolism pathway, respectively. Solid arrows indicate that the reaction proceeds continuously, dotted arrows indicate that intermediate metabolites are omitted. 1235 and 1246 represent Sample 1, Sample 2, Sample 3 and Sample 5 of control group (1235 route) and Sample 1, Sample 2, Sample 4 and Sample 6 of treatment group (1246 route), respectively. Sample 1, Sample 2 and Sample 3 were the heterotrophic cells at 100 h, 250 h, and 550 h, respectively; Sample 4 was Sample 2 cells induction for 0.5 day; Sample 5 was Sample 3 cells induction for 6 days; Sample 6 was the Sample 2 cells induction for 6 days. The number of replications is two ($n=2$)

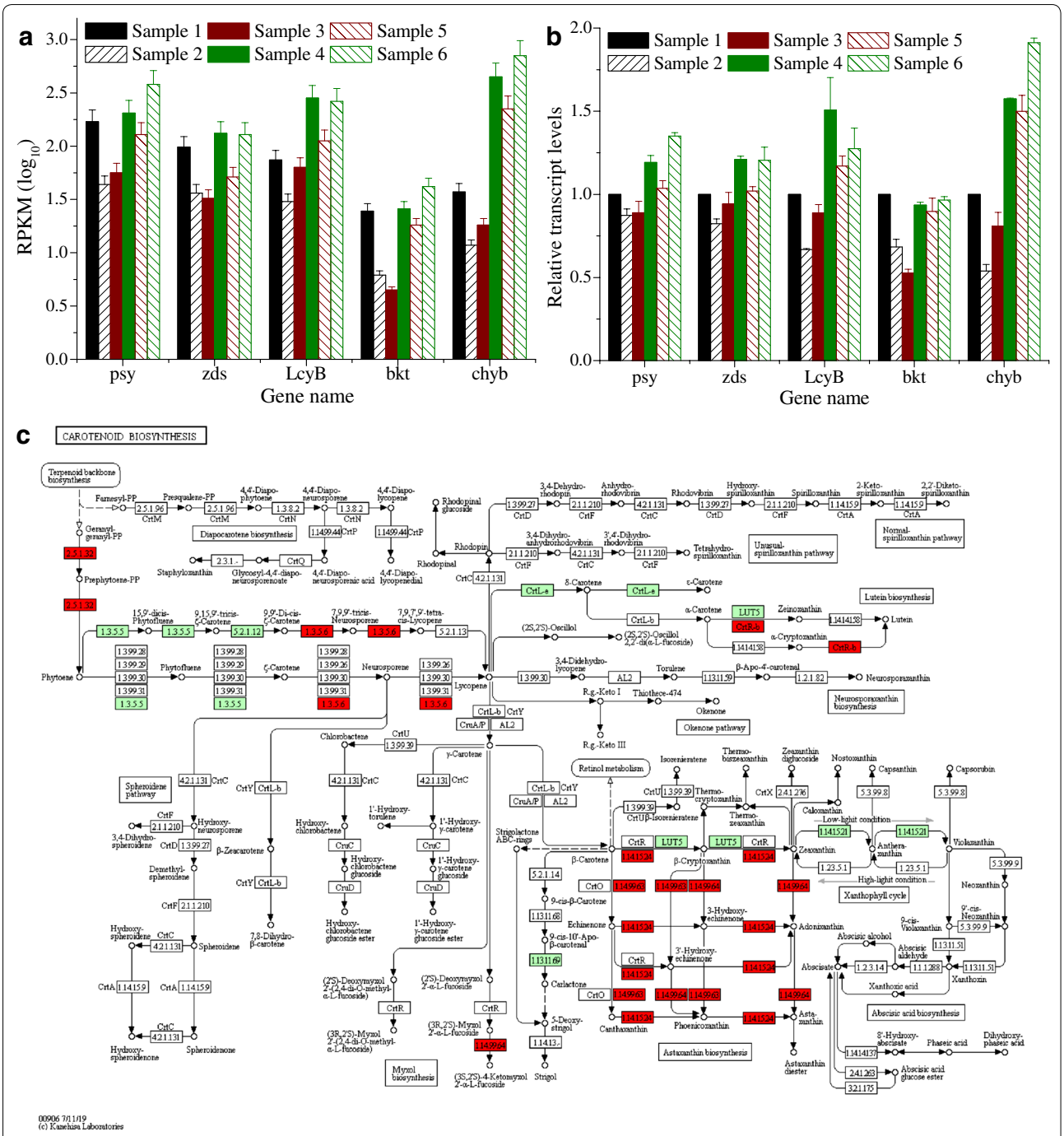

Fig. 5 RPKM and unigene transcription changes involved in astaxanthin biosynthesis pathways of *H. pluvialis*. **a**, **b** represent RPKM changes (**a**) and relative transcript level changes (**b**) involved in astaxanthin biosynthesis pathways of *H. pluvialis* in control group (1235 route) and treatment group (1246 route), respectively. To calculate genes transcript level, Sample 1 was regarded as control; comparing with control group (1235 route), the gene transcription changes of the treatment group (1246 route) were presented in KEGG pathway (**c**). Sample 1, Sample 2 and Sample 3 were the heterotrophic cells at 100 h, 250 h, and 550 h, respectively; Sample 4 was Sample 2 cells induction for 0.5 day; Sample 5 was Sample 3 cells induction for 6 days; Sample 6 was the Sample 2 cells induction for 6 days. Data shown as mean ± SD, and number of replications is two ($n = 2$)

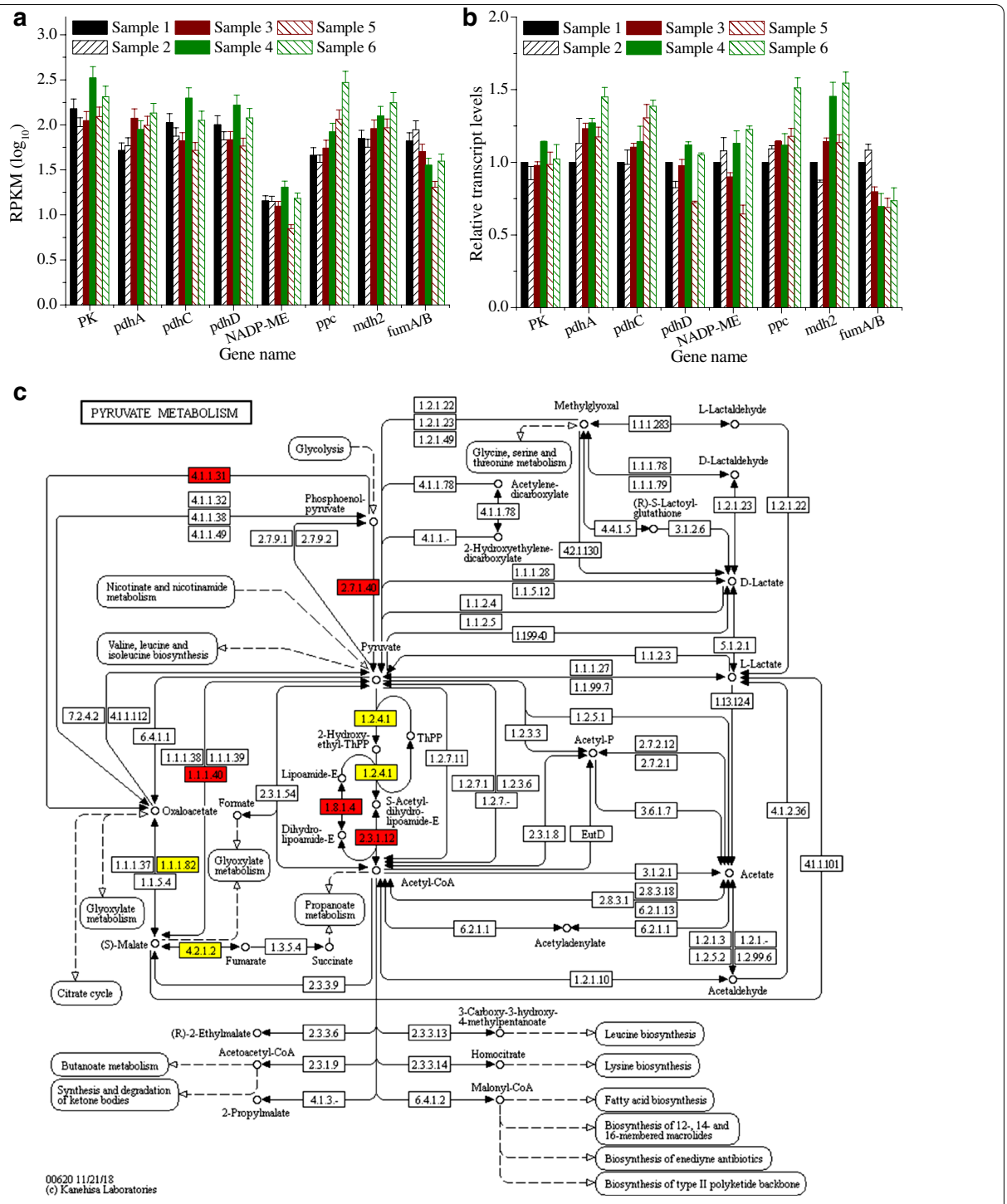

Fig. 6 RPKM and unigene transcription changes involved in pyruvate metabolism pathways of *H. pluvialis*. **a**, **b** represent RPKM changes (**a**) and relative transcript level changes (**b**) involved in pyruvate biosynthesis pathways of *H. pluvialis* in control group (1235 route) and treatment group (1246 route), respectively. To calculate genes transcript level, Sample 1 was regarded as control; comparing with control group, the gene transcription changes of the treatment group were presented in KEGG pathway (**c**). Sample 1, Sample 2 and Sample 3 were the heterotrophic cells at 100 h, 250 h, and 550 h, respectively; Sample 4 was Sample 2 cells induction for 0.5 day; Sample 5 was Sample 3 cells induction for 6 days; Sample 6 was the Sample 2 cells induction for 6 days. Yellow represents both down- and up-regulation gene, and red represents upregulation gene. Data shown as mean ± SD, and number of replications is two ($n = 2$)

et al. (2016) and He et al. (2018) also reported that the upregulation of *lcyB* was accompanied by the downregulation of *lcyE*.

Transcriptome and pathway analysis involved in pyruvate metabolism

In most microalgae, the direct product of photosynthesis is glucose. Then, glucose will be converted into lipid (Melis 2012). The dehydration condensation between lipid and free astaxanthin formed esterified form astaxanthin (Karsten et al. 2009; Schoefs et al. 2001). Astaxanthin esterification drove the formation and accumulation of astaxanthin (Chen et al. 2015). Pyruvate metabolism plays a major role in shifting carbon from glucose toward lipid synthesis (Chen et al. 2009; Orly et al. 2015). Pyruvate can interact with 3-phosphoglycerol aldehyde, yielding the substrate for producing isopentenyl pyrophosphate (IPP) through non-mevalonate pathway or mevalonate pathway (Saakov 2005; Ye et al. 2008). IPP is the precursor for astaxanthin synthesis (Lichtenthaler 1999). As such, pyruvate metabolism plays an important role in astaxanthin synthesis.

Pyruvate kinase (PK), a final enzyme of glycolysis, irreversibly converts phosphoenolpyruvate (PEP) into pyruvate with the concurrent generation of ATP (Shtaida et al. 2015). Compared with control, the transcription level of *pk* gene was 1.3-fold up-regulated at the end of photoinduction (Table 1). Chen also reported that the increase of esterified form astaxanthin synthesis was accompanied by a 3.5-fold increase in *pk* (Cheng et al. 2017). Acetyl-CoA is the precursor for lipid synthesis. Pyruvate would be converted into acetyl-CoA, catalyzed by pyruvate dehydrogenase complex (PDH) (Li et al. 2014). Intriguingly, the upregulation of pyruvate dehydrogenase E1 component alpha subunit (pdhA), pyruvate dehydrogenase E2 component (pdhC), dihydrolipoamide dehydrogenase (pdhD) were observed when akinetes formation was used non-motile as seeds; whereas, in control only *pdhA* gene was up-regulated (Fig. 6a, b). Therefore, compared with control, non-motile cells have stronger pyruvate metabolism ability.

Additionally, malate dehydrogenase (oxaloacetate-decarboxylating) (NADP+) (NADP-ME) supplies carbon and NADPH for de novo fatty acid production. Compared with control, *NADP-ME* was up-regulated by 1.8-fold at the end of photoinduction (Table 1). Phosphoenolpyruvate carboxylase (PPC), which catalyzes PEP to oxaloacetate, was 2.1-fold up-regulated at the end of photoinduction (Table 1). The increased transcription level of malate dehydrogenase (NADP+) (MDH) accelerates the conversion of malate from oxaloacetate, thus providing additional carbon and NADPH for de novo fatty acid production (Shtaida et al. 2015). At the end of photoinduction, *MDH* was up-regulated by 1.5-fold when used non-motile cells as seeds (Table 1).

Compared with control, all genes related to pyruvate metabolism have a higher gene transcription level at the end of induction (Fig. 6c and Table 1). Above all, transcriptome analysis results further indicated that non-motile cells have stronger pyruvate metabolism ability. Whereas, pyruvate metabolism plays an important role in astaxanthin synthesis. The results further explained that non-motile cells have a strong ability to accumulate astaxanthin. The high astaxanthin synthesis ability of non-motile cells was ascribed to the high transcription level of genes related with pyruvate metabolism.

Conclusions

Above all, astaxanthin synthesis is closely related to pyruvate metabolism. The strong ability of non-motile cells to accumulate astaxanthin can be attributed to the improvement of pyruvate metabolism. The results are expected to further guide the in-depth optimization of the astaxanthin production process in *H. pluvialis*.

Supplementary information

Supplementary information accompanies this paper at https://doi.org/10.1186/s40643-019-0293-1.

Additional file 1: Table S1. Gene specific primers of qRT-PCR.

Abbreviations

DEGs: differentially expressed genes; PE: paired-end; NODE: National Omics Data Encyclopedia; GGPP: geranylgeranyl-pp; GA3: gibberellin; SEM: scanning electron microscope; TEM: transmission electron microscope.

Acknowledgements

Not applicable.

Authors' contributions

MW and LF designed the study; LF analyzed the data and drafted the manuscript; JZ and ZF prepared the transcriptome sequencing samples and electron microscopy samples; MW reviewed and edited the article. All authors read and approved the final manuscript.

Funding

This research was funded by National Natural Science Foundation of China (31500062), China, Post Doctoral Science Foundation (2013M530183 and 2014T70400), China, and the Fundamental Research Funds for the Central Universities (222201414024), China. The authors declared that they have no conflicts of interest to this work.

Availability of data and materials

The datasets supporting the conclusions of this article are included in the main manuscript file and additional files.

Ethics approval and consent to participate

Not applicable.

Consent for publication

Not applicable.

Competing interests
The authors declare that they have no competing interests.

Received: 9 October 2019 Accepted: 30 December 2019
Published online: 24 January 2020

References

Borowitzka MA, Huisman JM, Osborn A (1991) Culture of the astaxanthin-producing green alga *Haematococcus pluvialis* 1. Effects of nutrients on growth and cell type. J Appl Phycol 3:295–304

Chen T, Wei D, Chen G, Wang Y, Chen F (2009) Employment of organic acids to enhance astaxanthin formation in heterotrophic *Chlorella zofingiensis*. J Food Process Preserv 33:271–284

Chen G, Wang B, Han D, Sommerfeld M, Lu Y, Chen F, Hu Q (2015) Molecular mechanisms of the coordination between astaxanthin and fatty acid biosynthesis in *Haematococcus pluvialis* (Chlorophyceae). Plant J 81:95–107

Cheng J, Li K, Zhu Y, Yang W, Zhou J, Cen K (2017) Transcriptome sequencing and metabolic pathways of astaxanthin accumulated in *Haematococcus pluvialis* mutant under 15% CO_2. Bioresour Technol 228:99–105

Choi YE, Yun YS, Park JM, Yang JW (2011) Determination of the time transferring cells for astaxanthin production considering two-stage process of *Haematococcus pluvialis* cultivation. Bioresour Technol 102:11249–11253

Gao Z, Meng C, Zhang X, Xu D, Miao X, Wang Y, Yang L, Lv H, Chen L, Ye N (2012a) Induction of salicylic acid (SA) on transcriptional expression of eight carotenoid genes and astaxanthin accumulation in *Haematococcus pluvialis*. Enzyme Microb Technol 51:225–230

Gao Z, Meng C, Zhang X, Xu D, Zhao Y, Wang Y, Lv H, Liming Y, Chen L, Ye N (2012b) Differential expression of carotenogenic genes, associated changes on astaxanthin production and photosynthesis features induced by JA in *H. pluvialis*. PLoS ONE 7:e42243

Gao Z, Meng C, Gao H, Li Y, Zhang X, Xu D, Zhou S, Liu B, Su Y, Ye N (2013) Carotenoid genes transcriptional regulation for astaxanthin accumulation in fresh water unicellular alga *Haematococcus pluvialis* by gibberellin A3 (GA3). Indian J Biochem Biophys 50:548–553

Gao Z, Miao X, Zhang X, Wu G, Guo Y, Wang M, Li B, Li X, Gao Y, Hu S, Sun J, Cui J, Meng C, Li Y (2016) Comparative fatty acid transcriptomic test and iTRAQ-based proteomic analysis in *Haematococcus pluvialis* upon salicylic acid (SA) and jasmonic acid (JA) inductions. Algal Res 17:277–284

García-Malea MC, Acién FG, Fernández JM, Cerón MC, Molina E (2006) Continuous production of green cells of *Haematococcus pluvialis*: modeling of the irradiance effect. Enzyme Microb Technol 38:981–989

Gu W, Xie X, Gao S, Zhou W, Pan G, Wang G (2013) Comparison of different cells of *Haematococcus pluvialis* reveals an extensive acclimation mechanism during its aging process: from a perspective of photosynthesis. PLoS ONE 8:e67028

Hata N, Ogbonna JC, Hasegawa Y, Taroda H, Tanaka H (2001) Production of astaxanthin by *Haematococcus pluvialis* in a sequential heterotrophic-photoautotrophic culture. J Appl Phycol 13:395–402

He P, Duncan J, Barber J (2007) Astaxanthin accumulation in the green alga *Haematococcus pluvialis*: effects of cultivation parameters. J Integr Plant Biol 49:447–451

He B, Hou L, Dong M, Shi J, Huang X, Ding Y, Cong X, Zhang F, Zhang X, Zang X (2018) Transcriptome analysis in *Haematococcus pluvialis*: astaxanthin induction by high light with acetate and Fe(2). Int J Mol Sci 19:175–193

Huang JC, Chen F, Sandmann G (2006) Stress-related differential expression of multiple *β*-carotene ketolase genes in the unicellular green alga *Haematococcus pluvialis*. J Biotechnol 122:176–185

Huerlimann R, Heimann K (2013) Comprehensive guide to acetyl-carboxylases in algae. Crit Rev Biotechnol 33:49–65

Kang CD, Lee JS, Park TH, Sim SJ (2005) Comparison of heterotrophic and photoautotrophic induction on astaxanthin production by *Haematococcus pluvialis*. Appl Microbiol Biotechnol 68:237–241

Karsten H, Maximilian K, Jens R, Paul S, Graeme N, Klaus A (2009) Determination of astaxanthin and astaxanthin esters in the microalgae *Haematococcus pluvialis* by LC-(APCI)MS and characterization of predominant carotenoid isomers by NMR spectroscopy. Anal Bioanal Chem 395:1613–1622

Lee C, Choi YE, Yun YS (2016) A strategy for promoting astaxanthin accumulation in *Haematococcus pluvialis* by 1-aminocyclopropane-1-carboxylic acid application. J Biotechnol 236:120–127

Levitan O, Dinamarca J, Zelzion E, Lun DS, Guerra LT, Kim MK, Kim J, Van Mooy BA, Bhattacharya D, Falkowski PG (2015) Remodeling of intermediate metabolism in the diatom *Phaeodactylum tricornutum* under nitrogen stress. Proc Natl Acad Sci USA 112:412–417

Li J, Han D, Wang D, Ning K, Jia J, Wei L, Jing X, Huang S, Chen J, Li Y (2014) Choreography of transcriptomes and lipidomes of *Nannochloropsis* reveals the mechanisms of oil synthesis in microalgae. Plant Cell 26:1645–1665

Li K, Cheng J, Lu H, Yang W, Zhou J, Cen K (2017) Transcriptome-based analysis on carbon metabolism of *Haematococcus pluvialis* mutant under 15% CO_2. Bioresour Technol 233:313–321

Li F, Cai M, Lin M, Huang X, Wang J, Zheng X, Wu S, An Y (2019a) Accumulation of astaxanthin was improved by the nonmotile cells of *Haematococcus pluvialis*. Biomed Res Int 2019:8101762

Li Q, Zhang L, Liu J (2019b) Comparative transcriptome analysis at seven time points during *Haematococcus pluvialis* motile cell growth and astaxanthin accumulation. Aquaculture 503:304–311

Lichtenthaler HK (1999) The 1-deoxy-d-xylulose-5-phosphate pathway of isoprenoid biosynthesis in plants. Annu Rev Plant Physiol Plant Mol Biol 50:47–65

Linden H (1999) Carotenoid hydroxylase from *Haematococcus pluvialis*: cDNA sequence, regulation and functional complementation. Biochim Biophys Acta 1446:203–212

Livak K, Schmittgen T (2000) Analysis of Relative Gene Expression Data Using Real-Time Quantitative PCR and the $2^{-\Delta\Delta Ct}$ Method. Methods 25:402–408

Lorenz RT, Cysewski GR (2000) Commercial potential for *Haematococcus* microalgae as a natural source of astaxanthin. Trends Biotechnol 18:160–167

Lv H, Xia F, Liu M, Cui X, Wahid F, Jia S (2016) Metabolomic profiling of the astaxanthin accumulation process induced by high light in *Haematococcus pluvialis*. Algal Res 20:35–43

Melis A (2012) Photosynthesis-to-fuels: from sunlight to hydrogen, isoprene, and botryococcene production. Energy Environ Sci 5:5531–5539

Olaizola M (2000) Commercial production of astaxanthin from *Haematococcus pluvialis* using 25,000-liter outdoor photobioreactors. J Appl Phycol 12:499–506

Ranjbar R, Inoue R, Shiraishi H, Katsuda T, Katoh S (2008) High efficiency production of astaxanthin by autotrophic cultivation of *Haematococcus pluvialis* in a bubble column photobioreactor. Biochem Eng J 39:575–580

Saakov VS (2005) Pools of 14 C-malic acid as a substrate for pyruvate production for the DOXP/MEP pathway of biosynthesis of carotenoids in chloroplasts. Dokl Biochem Biophys 400:7–13

Sarada R, Tripathi U, Ravishankar GA (2002) Influence of stress on astaxanthin production in *Haematococcus pluvialis* grown under different culture conditions. Process Biochem 37:623–627

Schoefs B, Rmiki N, Rachadi J, Lemoine Y (2001) Astaxanthin accumulation in *Haematococcus* requires a cytochrome P450 hydroxylase and an active synthesis of fatty acids. FEBS Lett 500:125–128

Shtaida N, Khozin-Goldberg I, Boussiba S (2015) The role of pyruvate hub enzymes in supplying carbon precursors for fatty acid synthesis in photosynthetic microalgae. Photosynthesis Res 125:407–422

Wan M, Hou D, Li Y, Fan J, Huang J, Liang S, Wang W, Pan R, Wang J, Li S (2014a) The effective photoinduction of *Haematococcus pluvialis* for accumulating astaxanthin with attached cultivation. Bioresour Technol 163:26–32

Wan M, Zhang J, Hou D, Fan J, Li Y, Huang J, Wang J (2014b) The effect of temperature on cell growth and astaxanthin accumulation of *Haematococcus pluvialis* during a light-dark cyclic cultivation. Bioresour Technol 167:276–283

Wan M, Zhang Z, Wang J, Huang J, Fan J, Yu A, Wang W, Li Y (2015) Sequential Heterotrophy–Dilution–Photoinduction Cultivation of *Haematococcus pluvialis* for efficient production of astaxanthin. Bioresour Technol 198:557–563

Wang J, Sommerfeld MR, Lu C, Hu Q (2013) Combined effect of initial biomass density and nitrogen concentration on growth and astaxanthin production of *Haematococcus pluvialis* (Chlorophyta) in outdoor cultivation. Algae 28:193–202

Wen Z, Liu Z, Hou Y, Liu C, Gao F, Zheng Y, Chen F (2015) Ethanol induced astaxanthin accumulation and transcriptional expression of carotenogenic genes in *Haematococcus pluvialis*. Enzyme Microb Technol 78:10–17

Ye ZW, Jiang JG, Wu GH (2008) Biosynthesis and regulation of carotenoids in *Dunaliella*: progresses and prospects. Biotechnol Adv 26:352–360

Yu X, Niu X, Zhang X, Pei G, Liu J, Chen L, Zhang W (2015) Identification and mechanism analysis of chemical modulators enhancing astaxanthin accumulation in *Haematococcus pluvialis*. Algal Res 11:284–293

Zhang BY, Geng YH, Li ZK, Hu HJ, Li YG (2009) Production of astaxanthin from *Haematococcus* in open pond by two-stage growth one-step process. Aquaculture 295:275–281

Zhong YJ, Huang JC, Liu J, Li Y, Jiang Y, Xu ZF, Sandmann G, Chen F (2011) Functional characterization of various algal carotenoid ketolases reveals that ketolating zeaxanthin efficiently is essential for high production of astaxanthin in transgenic Arabidopsis. J Exp Bot 62:3659–3669

Publisher's Note